

U boson searches at KLOE

The KLOE-2 Collaboration

F. Archilli,^{n,o} D. Babusci,^f D. Badoni,^{n,o} I. Balwierz,^e G. Bencivenni,^f
 C. Bini,^{l,m} C. Bloise,^f V. Bocci,^m F. Bossi,^f P. Branchini,^q
 A. Budano,^{p,q} S. A. Bulychjev,^g P. Campana,^f G. Capon,^f
 F. Ceradini,^{p,q} P. Ciambrone,^f E. Czerwiński,^f E. Dané,^f
 E. De Lucia,^f G. De Robertis,^b A. De Santis,^{l,m} G. De Zorzi,^{l,m}
 A. Di Domenico,^{l,m} C. Di Donato,^{h,i} D. Domenici,^f O. Erriquez,^{a,b}
 G. Fanizzi,^{a,b} G. Felici,^f S. Fiore,^{l,m} P. Franzini,^{l,m} P. Gauzzi,^{l,m}
 S. Giovannella,^f F. Gonnella,^{n,o} E. Graziani,^q F. Happacher,^f
 B. Höistad,^s E. Iarocci,^{j,f} M. Jacewicz,^s T. Johansson,^s V. Kulikov,^g
 A. Kupsc,^s J. Lee-Franzini,^{f,r} F. Loddo,^b M. Martemianov,^g
 M. Martini,^{f,k} M. Matsyuk,^g R. Messi,^{n,o} S. Miscetti,^f G. Morello,^f
 D. Moricciani,^o P. Moskal,^e F. Nguyen,^{p,q} A. Passeri,^q V. Patera,^{j,f}
 I. Prado Longhi,^{p,q} A. Ranieri,^b P. Santangelo,^f I. Sarra,^f
 M. Schioppa,^{c,d} B. Sciascia,^f A. Sciubba,^{j,f} M. Silarski,^e C. Taccini,^{p,q}
 L. Tortora,^q G. Venanzoni,^f R. Versaci,^{f,u} W. Wiślicki,^t M. Wolke,^s
 J. Zdebik.^e

^aDipartimento di Fisica dell'Università di Bari, Bari, Italy.

^bINFN Sezione di Bari, Bari, Italy.

^cDipartimento di Fisica dell'Università della Calabria, Cosenza, Italy.

^dINFN Gruppo collegato di Cosenza, Cosenza, Italy.

^eInstitute of Physics, Jagiellonian University, Cracow, Poland.

^fLaboratori Nazionali di Frascati dell'INFN, Frascati, Italy.

^gInstitute for Theoretical and Experimental Physics (ITEP), Moscow, Russia.

^hDipartimento di Fisica dell'Università "Federico II", Napoli, Italy.

ⁱINFN Sezione di Napoli, Napoli, Italy.

^jDipartimento di Scienze di Base ed Applicate per l'Ingegneria dell'Università "Sapienza",
 Roma, Italy.

^kDipartimento di Scienze e Tecnologie applicate, Università "Guglielmo Marconi", Roma, Italy.

^lDipartimento di Fisica dell'Università "Sapienza", Roma, Italy.

^mINFN Sezione di Roma, Roma, Italy.

ⁿDipartimento di Fisica dell'Università "Tor Vergata", Roma, Italy.

^oINFN Sezione di Roma Tor Vergata, Roma, Italy.

^pDipartimento di Fisica dell'Università "Roma Tre", Roma, Italy.

^qINFN Sezione di Roma Tre, Roma, Italy.

^rPhysics Department, State University of New York at Stony Brook, USA.

^sDepartment of Nuclear and Particle Physics, Uppsala University, Uppsala, Sweden.

^tA. Soltan Institute for Nuclear Studies, Warsaw, Poland.

^uPresent Address: CERN, CH-1211 Geneva 23, Switzerland.

Abstract. The existence of a secluded gauge sector could explain several puzzling astrophysical observations. This hypothesis can be tested at low energy e^+e^- colliders such as DAΦNE. Preliminary results obtained with KLOE data and perspectives for the KLOE-2 run, where a larger data sample is expected, are discussed.

1. Introduction

In recent years, several astrophysical observations have failed to find easy interpretations in terms of standard astrophysical and/or particle physics sources. A non exhaustive list of these observations includes the 511 keV gamma-ray signal from the galactic center observed by the INTEGRAL satellite [1], the excess in the cosmic ray positrons reported by PAMELA [2], the total electron and positron flux measured by ATIC [3], Fermi [4], and HESS [5, 6], and the annual modulation of the DAMA/LIBRA signal [7, 8].

An intriguing feature of these observations is that they suggest the existence of a WIMP dark matter particle belonging to a secluded gauge sector under which the Standard Model (SM) particles are uncharged [9, 10, 11, 12, 13, 14, 15, 16, 17, 18]. An abelian gauge field, the U boson with mass near the GeV scale, couples the secluded sector to the SM through its kinetic mixing with the SM hypercharge gauge field. The kinetic mixing parameter, ϵ , can naturally be of the order 10^{-4} – 10^{-2} . In a very minimal scenario, in addition to the U , it is natural to have a secluded Higgs boson, the h' , which spontaneously breaks the secluded gauge symmetry. A consequence of the above hypotheses is that observable effects can be induced in $\mathcal{O}(\text{GeV})$ -energy e^+e^- colliders [19, 20, 21, 22, 23, 24] and fixed target experiments [25, 26, 27, 28].

2. Searches for dark forces at KLOE

The KLOE experiment operates at DAΦNE, the e^+e^- Frascati ϕ -factory. From 2000 to 2006, KLOE collected 2.5 fb^{-1} of collisions at the ϕ meson peak and about 240 pb^{-1} below the ϕ resonance ($\sqrt{s} = 1 \text{ GeV}$). The ϕ meson predominantly decays into charged and neutral kaons, thus allowing KLOE to make precision studies in the fields of flavor physics, low energy QCD and test of discrete symmetries [29].

A new beam crossing scheme allowing a reduced beam size and increased luminosity is operating at DAΦNE [30]. The KLOE-2 detector was successfully installed in this new interaction region and has been upgraded with small angle tagging devices to detect both high and low energy electrons or positrons in $e^+e^- \rightarrow e^+e^-X$ events. About 5 fb^{-1} are expected in the first year of running. An inner tracker and small angle calorimeters are scheduled to be installed in a subsequent step, providing larger acceptance both for charged particles and photons. A detailed description of the KLOE-2 physics program can be found in Ref. [31].

The KLOE detector consists of a large cylindrical drift chamber, DC, surrounded by a lead-scintillating fiber electromagnetic calorimeter, EMC. A superconducting coil around the EMC provides a 0.52 T magnetic field. The all-stereo drift chamber [32], 4 m in diameter and 3.3 m long, is made of carbon fiber-epoxy composite and operates with a light gas mixture (90% helium, 10% isobutane). The position resolutions are $\sigma_{xy} \sim 150 \mu\text{m}$ and $\sigma_z \sim 2 \text{ mm}$. The momentum resolution is $\sigma(p_\perp)/p_\perp \approx 0.4\%$. Vertexes are reconstructed with a spatial resolution of $\sim 3 \text{ mm}$. The calorimeter [33] is divided into a barrel and two endcaps and covers 98% of the solid angle. The modules are read out at both ends by photomultipliers with a readout granularity of $\sim (4.4 \times 4.4) \text{ cm}^2$. The arrival times of particles and the positions in three dimensions of the energy deposits are obtained from the signals collected at the two ends. Cells close in time and space are grouped into a calorimeter cluster. The cluster energy E is the sum

of the cell energies. The cluster time T and position \vec{R} are energy weighted averages. Energy and time resolutions are $\sigma_E/E = 5.7\%/\sqrt{E \text{ (GeV)}}$ and $\sigma_t = 57 \text{ ps}/\sqrt{E \text{ (GeV)}} \oplus 50 \text{ ps}$, respectively.

The U boson can be produced at DAΦNE through radiative decays of neutral mesons, such as $\phi \rightarrow \eta U$. With the statistics already collected at KLOE, this decay can potentially probe couplings down to $\epsilon \sim 10^{-3}$ [21], covering most of the parameter's range of interest for the theory. The U boson can be observed by its decay into a lepton pair, while the η can be tagged by one of its not-rare decays.

Assuming also the existence of the h' , both the U and the h' can be produced at DAΦNE if their masses are smaller than M_ϕ . The mass of the U and h' are both free parameters, and the possible decay channels can be very different depending on which particle is heavier. In both cases, an interesting production channel is the h' -strahlung, $e^+e^- \rightarrow Uh'$ [19]. Assuming the h' to be lighter than the U boson, it turns out to be very long-lived, so that the signature process will be a lepton pair, generated by the U boson decay, plus missing energy. In the case $m_{h'} > m_U$, the dark higgs frequently decays to a pair of real or virtual U 's. In this case one can observe events with 6 leptons in the final state, due to the h' -strahlung process, or 4 leptons and a photon, due to the $e^+e^- \rightarrow h'\gamma$ reaction.

Another possible channel to look for the existence of the U boson is the $e^+e^- \rightarrow U\gamma$ process [19]. The expected cross section can be as high as $\mathcal{O}(\text{pb})$ at DAΦNE energies. The on-shell boson can decay into a lepton pair, giving rise to a $l^+l^-\gamma$ signal.

In the following, progresses on the analyses of $\phi \rightarrow \eta U$ and $e^+e^- \rightarrow Uh'$ channels are reported, together with perspectives for the new KLOE-2 run.

3. The $\phi \rightarrow \eta U$ decay

As discussed above, the search of the U boson can be performed at KLOE using the decay chain $\phi \rightarrow \eta U$, $U \rightarrow l^+l^-$. An irreducible background due to the Dalitz decay of the ϕ meson, $\phi \rightarrow \eta l^+l^-$, is present. This decay has been studied by SND and CMD-2 experiments, which measured a branching fraction of $BR(\phi \rightarrow \eta e^+e^-) = (1.19 \pm 0.19 \pm 0.07) \times 10^{-4}$ and $BR(\phi \rightarrow \eta e^+e^-) = (1.14 \pm 0.10 \pm 0.06) \times 10^{-4}$ respectively [34, 35]. This corresponds to a cross section of $\sigma(\phi \rightarrow \eta l^+l^-) \sim 0.7 \text{ nb}$, while for the signal

$$\sigma(\phi \rightarrow \eta U) = \epsilon^2 |F_{\phi\eta}(m_U^2)|^2 \frac{\lambda^{3/2}(m_\phi^2, m_\eta^2, m_U^2)}{\lambda^{3/2}(m_\phi^2, m_\eta^2, 0)} \sigma(\phi \rightarrow \eta\gamma) \sim 40 \text{ fb} \quad (1)$$

using $\epsilon = 10^{-3}$, $|F_{\phi\eta}(m_U^2)|^2 = 1$. In Eq. (1), $|F_{\phi\eta}(m_U^2)|^2$ is the form factor of the $\phi \rightarrow \eta\gamma$ decay evaluated at the U mass while the following term represent the ratio of the kinematic functions of the involved decays. Despite the values of the cross section, the different shapes of the e^+e^- invariant mass for the two processes allow to test the ϵ parameter down to 10^{-3} with the whole KLOE data set [21].

The best channel to search for the $\phi \rightarrow \eta U$ process at KLOE is the $U \rightarrow e^+e^-$ decay for two reasons: (i) a wider range of U boson mass can be tested; (ii) e^\pm are easily identified using the time-of-flight (ToF) measurement. The η can be tagged by the three-pion or two-photon final state, which represent $\sim 85\%$ of the total decay rate. We have performed a preliminary analysis using the $\eta \rightarrow \pi^+\pi^-\pi^0$ channel, which provide a clean signal with four charged tracks and two photon in the final state. Studies are under way also for the $\eta \rightarrow \gamma\gamma$ sample.

3.1. The $\eta \rightarrow \pi^+\pi^-\pi^0$ final state

The preliminary analysis of the $\eta \rightarrow \pi^+\pi^-\pi^0$ final state has been performed on 1.5 fb^{-1} . Preselection cuts require: (i) four tracks in a cylinder around the interaction point (IP) plus two photon candidates; (ii) best $\pi^+\pi^-\gamma\gamma$ match to the η mass using the pion hypothesis for tracks; (iii) other two tracks assigned to e^+e^- ; (iv) loose cuts on η and π^0 invariant masses

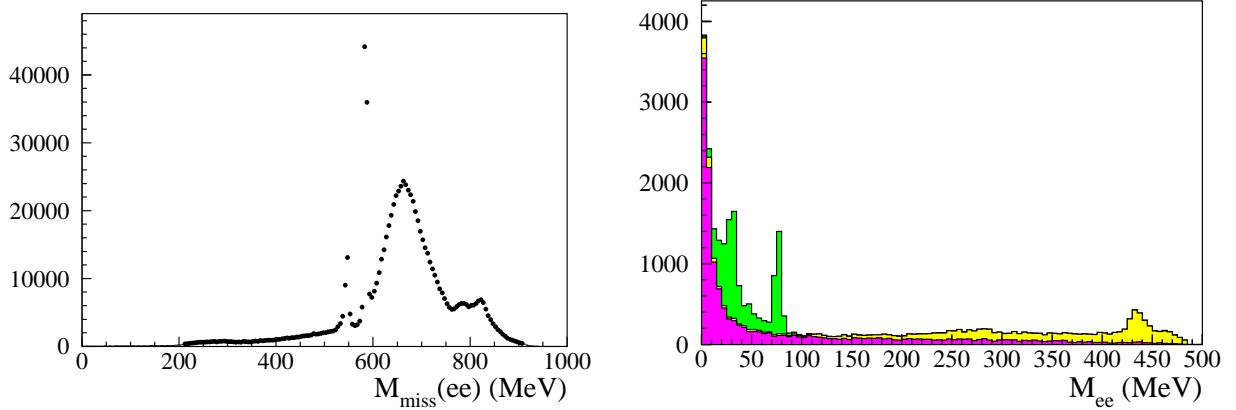


Figure 1. Left: missing mass of the e^+e^- pair for data sample after preselection cuts. The $\phi \rightarrow \eta e^+e^-$ signal is clearly visible in the peak corresponding to η mass. The second peak at ~ 590 MeV is due to $K_S \rightarrow \pi^+\pi^-$ events with wrong mass assignment. Right: M_{ee} distribution for data at different analysis steps: preselection (green), conversion (yellow) and ToF (purple) cuts.

($495 < M_{\pi^+\pi^-\gamma\gamma} < 600$ MeV, $70 < M_{\gamma\gamma} < 200$ MeV). These simple cuts allow to clearly see the peak due to $\phi \rightarrow \eta e^+e^-$ events in the distribution of the missing mass to the e^+e^- pair, $M_{\text{miss}}(ee)$ (see Fig. 1-left). A cut $535 < M_{\text{miss}}(ee) < 560$ MeV is then applied.

A residual background contamination, due to $\phi \rightarrow \eta\gamma$ events with photon conversion on beam pipe (BP) or drift chamber walls (DCW), is rejected by tracking back to BP/DCW surfaces the two e^+ , e^- candidates and then reconstructing the electron-positron invariant mass (M_{ee}) and the distance between the two particles (D_{ee}). Both quantities are small if coming from photon conversion. $\phi \rightarrow K\bar{K}$ and $\phi \rightarrow \pi^+\pi^-\pi^0$ events surviving analysis cuts have more than two pions in the final state. They are rejected using time-of-flight to the calorimeter. When an EMC cluster is connected to a track, the arrival time to the calorimeter is evaluated both with calorimeter (T_{cluster}) and drift chamber (T_{track}) information. Events with an e^+ , e^- candidate outside a 3σ 's window on the $DT = T_{\text{track}} - T_{\text{cluster}}$ variables are rejected. In Fig. 1-right the M_{ee} distribution evaluated at IP for data at different steps of the analysis is shown. The conversion and ToF cuts remove events at low and high invariant mass values respectively.

In Fig. 2 the comparison between data and Monte Carlo (MC) events for M_{ee} and $\cos\psi^*$ distributions is shown. The second variable is the angle between the η and the e^+ in the e^+e^- rest frame. About 14,000 $\phi \rightarrow \eta e^+e^-$, $\eta \rightarrow \pi^+\pi^-\pi^0$ candidates are present in the analyzed data set, with a negligible residual background contamination. The MC description of these kind of events is done using Vector Meson Dominance, and the form factor slope parameter is taken from the measurement of SND experiment, obtained with 213 events [34]. Since an accurate description of the irreducible background is important for the search of the $\phi \rightarrow \eta U$ signal, we extract it directly from our data. The decay parametrization is taken from Ref. [36]:

$$\frac{d}{dq^2} \frac{\Gamma(\phi \rightarrow \eta e^+e^-)}{\Gamma(\phi \rightarrow \eta\gamma)} = \frac{\alpha}{3\pi} \frac{|F_{\phi\eta}(q^2)|^2}{q^2} \sqrt{1 - \frac{4m^2}{q^2}} \left(1 + \frac{2m^2}{q^2}\right) \left[\left(1 + \frac{q^2}{m_\phi^2 - m_\eta^2}\right)^2 - \frac{4m_\phi^2 q^2}{(m_\phi^2 - m_\eta^2)^2} \right]^{3/2} \quad (2)$$

$$F(q_{\phi\eta}^2) = \frac{1}{1 - q^2/\Lambda_{\phi\eta}^2} \quad (3)$$

The preliminary fit to the M_{ee} shape, reported in Fig. 3, has $\chi^2/\text{ndf} = 2.1\%$. The resulting accuracy on form factor slope, $b = \Lambda_{\phi\eta}^{-2}$, is 2.8%. Smearing matrix has not been included.

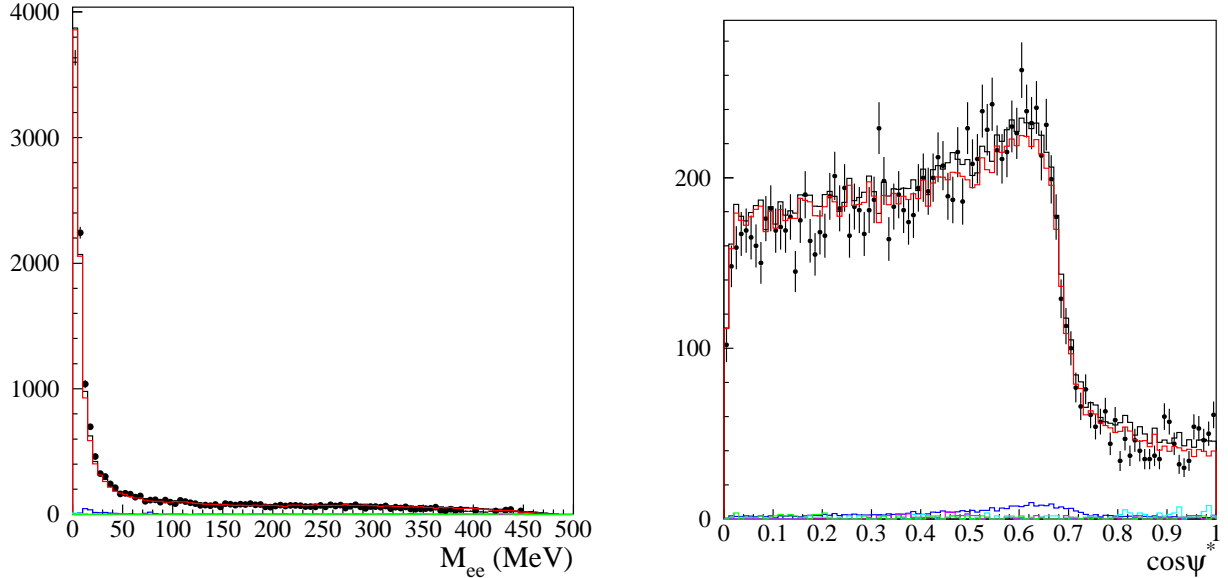


Figure 2. Invariant mass of the e^+e^- pair (left) and $\cos\psi^*$ distribution (right) for $\phi \rightarrow \eta e^+e^-$, $\eta \rightarrow \pi^+\pi^-\pi^0$ events. Dots are data, the red line represents the expected MC shape for signal while the residual background contamination from ϕ decays is shown in blue. The black solid line is the sum of all MC contributions.

The $\phi \rightarrow \eta U$ MC signal has been produced according to Ref. [21], with a flat distribution of the e^+e^- invariant mass. Events are then divided in sub-samples of 1 MeV width. For each M_{ee} value, signal hypothesis has been excluded at 90% C.L. using the CL_S technique [37]. For the $\phi \rightarrow \eta U$ signal, the opening of the $U \rightarrow \mu^+\mu^-$ threshold has been included, in the hypothesis that the U boson decays only to lepton pairs with $\Gamma(U \rightarrow e^+e^-) = \Gamma(U \rightarrow \mu^+\mu^-)$. The expected shape for the irreducible background $\phi \rightarrow \eta e^+e^-$ is obtained from our fit to the M_{ee} distribution, taking also into account the error on number of background events as a function of M_{ee} . In Fig. 4 the preliminary exclusion plot on $\alpha'/\alpha = \epsilon^2$ variable is compared with recent measurements from BABAR [39] and MAMI [40] experiments. Our result greatly improves existing limits in the mass region $60 < M_{ee} < 210$ MeV, and it is also interesting at larger masses, where existing upper limits rely on different assumptions.

3.2. The $\eta \rightarrow \gamma\gamma$ final state

A similar analysis strategy has been developed for the decay chain $\phi \rightarrow \eta U$, $U \rightarrow e^+e^-$, $\eta \rightarrow \gamma\gamma$. The preselection requires: (i) two tracks coming from a cylinder around IP, classified as e^\pm using ToF information; (ii) two photon candidates; (iii) the cosine of the angle between photons in η rest frame to be ~ 1 ; (iv) a loose cut on the total invariant mass of the system, $950 < M_{\text{tot}} < 1150$ MeV.

The most severe background is generated by double radiative Bhabha scattering events and it is strongly reduced by cutting on the opening angle between the charged tracks and the photons. Residual non-Bhabha background is rejected by using further electron identification, based on the E/p ratio for the e^+e^- candidates. The resulting background reduction is still not enough for the search of $\phi \rightarrow \eta U$ events. The M_{ee} spectrum obtained with 1.7 fb^{-1} shows a clear evidence of $\phi \rightarrow \eta e^+e^-$ Dalitz decays at low values and some residual background contamination at high M_{ee} due to Bhabha events. Work is in progress to further improve signal to background ratio.

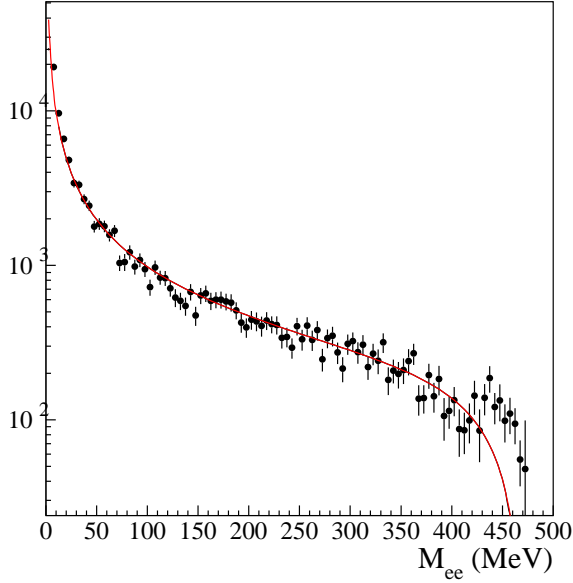


Figure 3. Fit to the M_{ee} spectrum for the Dalitz decays $\phi \rightarrow \eta e^+e^-$, using the $\eta \rightarrow \pi^+\pi^-\pi^0$ final state.

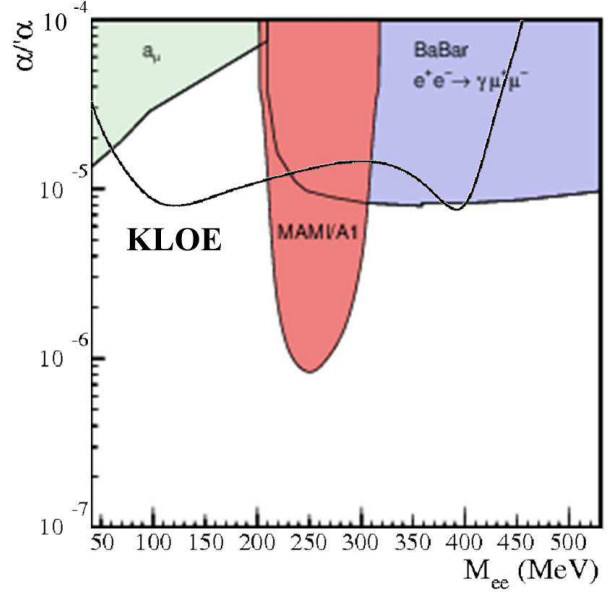


Figure 4. Exclusion plot for the parameter $\alpha'/\alpha = \epsilon^2$, compared with other existing measurements.

4. The higgs'-strahlung channel

The feasibility of the search for the process $e^+e^- \rightarrow Uh'$ has been done considering the $m_{h'} < m_U$ case. At DAΦNE energies, for $\epsilon \sim 10^{-3}$, a production cross section of ≈ 20 fb is expected and the h' has $\tau_{h'} > 10 \mu\text{s}$, escaping the detection. The signature is therefore a lepton pair from the U boson plus missing energy.

The selection strategy has been optimized using Monte Carlo events. The signal has been generated according to Ref. [19] in a discrete set of mass values in the range $m_U \leq 900$ MeV, $m_{h'} \leq 400$ MeV. The $U \rightarrow e^+e^-$ events are not selected by any official KLOE event classification (ECL) algorithms, which divide the events on the basis of topological information and provide reconstructed data to be used for different analyses. On the contrary, ECL is fully efficient for $U \rightarrow \mu^+\mu^-$ events when $m_{h'} < 300$ MeV. We therefore considered the $\mu^-\mu^-$ final state only.

Muons are identified and separated from electrons and pions using a neural network algorithm based on energy depositions along the shower depth in the calorimeter and E/p , β variables. The other relevant cuts to reduce background contamination are: (i) missing momentum direction in the barrel calorimeter; (ii) a tight cut on vertex-IP distance and (iii) no clusters in the calorimeter, with the exception of the two associated to tracks. The residual background contamination is due to $e^+e^- \rightarrow \pi^+\pi^-\gamma/\mu^-\mu^-\gamma$ continuum events with an undetected photon, and to $\phi \rightarrow K^+K^- \rightarrow \mu + \mu^-\nu\bar{\nu}$ with early decaying kaons.

In Fig. 5-left the distribution of the recoil mass to the $\mu^+\mu^-$ pair (M_{recoil}) as a function of the di-muon invariant mass obtained with 1.65 fb^{-1} is reported. M_{recoil} is evaluated using the center of mass energy of each run measured with Bhabha scattering events and the momenta of the muons. Continuum background, which can be further reduced tuning the π/μ identification algorithm, is concentrated in the band at $M_{\mu^+\mu^-} > 700$ MeV. The $\phi \rightarrow K^+K^-$ channel covers a wider region of the plane ($M_{\mu^+\mu^-} < 600$ MeV, $M_{\text{recoil}} < 300$ MeV). This background, having only two muons in the final state and missing energy due to neutrinos, has the same signature of the signal. The efficiency for $e^+e^- \rightarrow Uh'$ events is 15–40%, depending on m_U , $m_{h'}$ masses. Taking into account the total integrated luminosity, a signal would show up as a sharp peak with ≤ 10 events in the $M_{\text{recoil}}-M_{\mu\mu}$ plane for $\epsilon \sim 10^{-3}$.

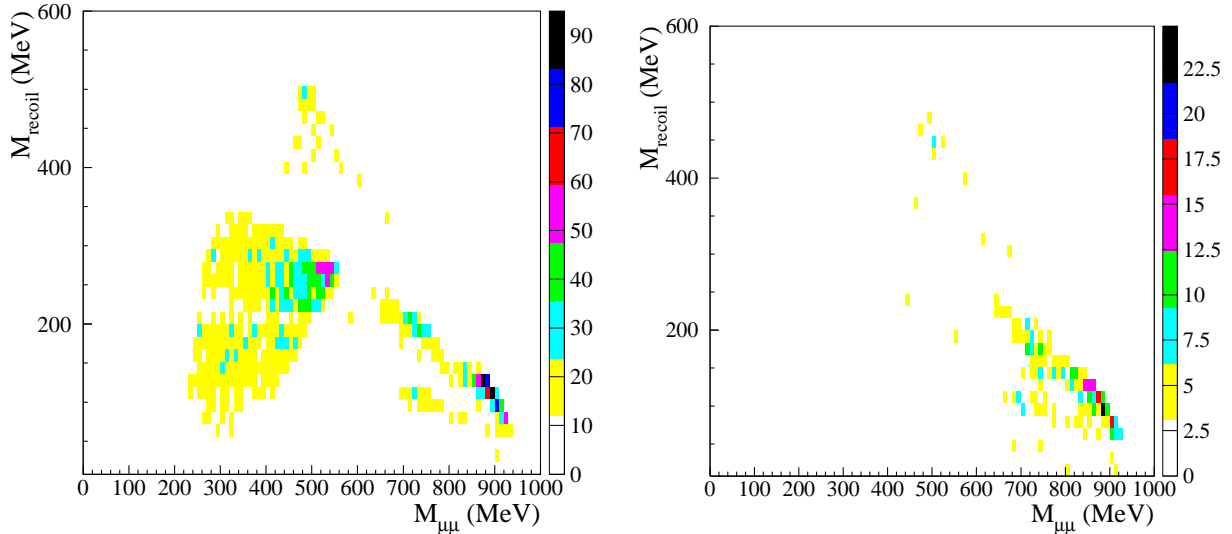


Figure 5. Search for $e^+e^- \rightarrow h'U$, $U \rightarrow \mu^+\mu^-$, $h' \rightarrow$ “invisible” events: recoil mass to the $\mu^+\mu^-$ pair as a function of the di-muon invariant mass for data taken at the ϕ mass (left) and at $\sqrt{s} = 1$ GeV (right).

Being the $\phi \rightarrow K^+K^-$ background a nasty background source, we repeated the analysis using the off-peak sample, 0.2 fb^{-1} taken at center of mass energy of 1 GeV. As can be seen in Fig. 5-right, the contribution from resonant background is not present anymore, providing a much cleaner sample for the search of $e^+e^- \rightarrow Uh'$ candidates.

5. Summary and perspectives for KLOE-2

The search for $\phi \rightarrow \eta U$ with $\eta \rightarrow \pi^+\pi^-\pi^0$, using 1.5 fb^{-1} of KLOE data, results in a preliminary upper limit on the $\alpha'/\alpha = \epsilon^2$ parameter of $\approx 1 \times 10^{-5}$ @ 90% C.L. in a wide M_{ee} range. With a sample of $\mathcal{O}(20 \text{ fb}^{-1})$ expected at KLOE-2, this value can be improved to $\approx 3 \times 10^{-6}$ using the same η decay channel. The inclusion of other final states, such as $\eta \rightarrow \gamma\gamma$ and $\eta \rightarrow \pi^0\pi^0\pi^0$, will further improve this result.

The search of the higgs'-strahlung channel, $e^+e^- \rightarrow Uh'$ with $U \rightarrow \mu^+\mu^-$ plus missing energy, is limited by a non negligible $\phi \rightarrow K^+K^-$ background in a wide region of the $M_{\mu^+\mu^-}$, M_{recoil} plane. Work is in progress to reduce this contribution on the KLOE data sample. At KLOE-2, the improvement on the vertex resolution, achievable with the insertion of the inner tracker, will provide a higher rejection factor. The feasibility of a high statistics run at 1 GeV, where the resonant background contribution is naturally reduced, is also under discussion.

Acknowledgments

We thank the DAFNE team for their efforts in maintaining low background running conditions and their collaboration during all data-taking. We want to thank our technical staff: G. F. Fortugno and F. Sborzacchi for their dedication in ensuring efficient operation of the KLOE computing facilities; M. Anelli for his continuous attention to the gas system and detector safety; A. Balla, M. Gatta, G. Corradi and G. Papalino for electronics maintenance; M. Santoni, G. Paoluzzi and R. Rosellini for general detector support; C. Piscitelli for his help during major maintenance periods. This work was supported in part by EURODAPHNE, contract FMRX-CT98-0169; by the German Federal Ministry of Education and Research (BMBF) contract 06-KA-957; by the German Research Foundation (DFG), 'Emmy Noether Programme', contracts DE839/1-4; by the EU Integrated Infrastructure Initiative HadronPhysics Project under

contract number RII3-CT-2004-506078; by the European Commission under the 7th Framework Programme through the 'Research Infrastructures' action of the 'Capacities' Programme, Call: FP7-INFRASTRUCTURES-2008-1, Grant Agreement N. 227431; by the Polish Ministry of Science and Higher Education through the Grant No. 0469/B/H03/2009/37.

References

- [1] P. Jean *et al.*, *Astron. Astrophys.* 407, L55 (2003).
- [2] O. Adriani *et al.*, *Nature* 458, 607 (2009).
- [3] J. Chang *et al.*, *Nature* 456, 362 (2008).
- [4] A.A. Abdo *et al.*, *Phys. Rev. Lett.* 102, 181101 (2009).
- [5] F. Aharonian *et al.*, *Phys. Rev. Lett.* 101, 261104 (2008).
- [6] F. Aharonian *et al.*, *Astron. Astrophys.* 508, 561 (2009).
- [7] R. Bernabei *et al.*, *Int. J. Mod. Phys. D* 13, 2127 (2004).
- [8] R. Bernabei *et al.*, *Eur. Phys. J. C* 56, 333 (2008).
- [9] M. Pospelov, A. Ritz, M.B. Voloshin, *Phys. Lett. B* 662, 53 (2008).
- [10] N. Arkani-Hamed, D.P. Finkbeiner, T.R. Slatyer, N. Weiner, *Phys. Rev. D* 79, 015014 (2009).
- [11] D.S.M. Alves, S.R. Behbahani, P. Schuster, J.G. Wacker, *Phys. Lett. B* 692, 323 (2010).
- [12] M. Pospelov, A. Ritz, *Phys. Lett. B* 671, 391 (2009).
- [13] J. Hisano, S. Matsumoto, M.M. Nojiri, *Phys. Rev. Lett.* 92, 031303 (2004).
- [14] M. Cirelli, M. Kadastik, M. Raidal, A. Strumia, *Nucl. Phys. B* 813, 1 (2009).
- [15] J. March-Russell, S.M. West, D. Cumberbatch, D. Hooper, *JHEP* 07, 058 (2008).
- [16] I. Cholis, G. Dobler, D.P. Finkbeiner, L. Goodenough, N. Weiner, *Phys. Rev. D* 80, 123518 (2009).
- [17] I. Cholis, D.P. Finkbeiner, L. Goodenough, N. Weiner, *JCAP* 0912, 007 (2009).
- [18] N. Arkani-Hamed, N. Weiner, *JHEP* 12, 104 (2008).
- [19] B. Batell, M. Pospelov, A. Ritz, *Phys. Rev. D* 79, 115008 (2009).
- [20] R. Essig, P. Schuster, N. Toro, *Phys. Rev. D* 80, 015003 (2009).
- [21] M. Reece, L.T. Wang, *JHEP* 07, 051 (2009).
- [22] F. Bossi (2009), arXiv:0904.3815.
- [23] N. Borodatchenkova, D. Choudhury, M. Drees, *Phys. Rev. Lett.* 96, 141802 (2006).
- [24] P.F. Yin, J. Liu, S.h. Zhu, *Phys. Lett. B* 679, 362 (2009).
- [25] J.D. Bjorken, R. Essig, P. Schuster, N. Toro, *Phys. Rev. D* 80, 075018 (2009).
- [26] B. Batell, M. Pospelov, A. Ritz, *Phys. Rev. D* 80, 095024 (2009).
- [27] R. Essig, P. Schuster, N. Toro, B. Wojtsekhowski, *JHEP* 1102, 009 (2011).
- [28] M. Freytsis, G. Ovanessian, J. Thaler, *JHEP* 01, 111 (2010).
- [29] F. Bossi *et al.*, *Rivista del Nuovo Cimento*, Vol. 031, 531 (2008).
- [30] C. Milardi *et al.*, *ICFA Beam Dyn. Newslett.* 48, 23 (2009).
- [31] G. Amelino-Camelia *et al.*, *Eur. Phys. J. C* 68, 619 (2010).
- [32] M. Adinolfi *et al.*, *Nucl. Inst. and Meth. A* 488, 51 (2002).
- [33] M. Adinolfi *et al.*, *Nucl. Inst. and Meth. A* 482, 363 (2002).
- [34] M. N. Achasov *et al.*, *Phys. Lett. B* 504, 275 (2001).
- [35] R. R. Akhmetshin *et al.*, *Phys. Lett. B* 501, 191 (2001).
- [36] L.G. Landsberg, *Phys. Rep.* 128, 301 (1985).
- [37] T. Junk, *Nucl. Instr. Meth. A* 434, 435 (1999).
- [38] J.M. Bernardo and A.F.M. Smith, *Bayesian theory*, Wiley (2000).
- [39] B. Aubert *et al.*, *Phys. Rev. Lett.* 103 (2009) 081803.
- [40] H. Merkel *et al.*, *Phys. Rev. Lett.* 106 (2011) 251802.